

VSP Processing For Coal Reflections

Salman K Bubshait and Donald C. Lawton

ABSTRACT

Five VSP surveys were acquired in Alberta as part of a study of Mannville coals. The zero-offset VSP survey was processed using the VISTA software through to corridor stack and shows high reflection quality of P waves with no significant multiples in the data. Also, the three walkaway VSPs along different azimuths were processed through to the VSPCDP stage. A recommendation is suggested to have an overlap of a receiver in the borehole to minimize shot static errors. The walkaways displayed high reflection quality of both P and S waves that highlighted the Mannville coals. A slight improvement of the reflection of the coals is noticed in the SV waves over the P waves as offset increases.

INTRODUCTION

Vertical Seismic Profiling (VSP) is used to obtain several rock properties as well as to acquire a seismic image of the subsurface that helps with surface seismic interpretation and processing. Rock properties obtained from VSP surveys include velocity, attenuation, impedance and anisotropy. In addition, VSP surveys are used in the analysis of wave propagation (Stewart, 2001).

There are several ways in which a VSP survey is conducted. If a source is located tens of meters away from the borehole containing the receivers, then it is a “Zero Offset VSP Survey.” Also, if the source is shot at several offsets from the borehole, then it is called a “Walk-away VSP Survey” or “Multi-Offset VSP Survey.” In addition, if sources are at several azimuths from the borehole, the survey is called “Multi-Azimuth Survey.” All of the surveys mentioned provide 2D images of the subsurface. A 3D image also can be obtained with a full areal set of sources (Stewart, 2001).

The purpose of acquiring different VSP surveys depends on the goal of the survey. A zero offset VSP survey can provide information about the time-depth conversion, normal incidence reflectivity and interval velocities in depth. On the other hand, a multi-offset VSP survey could be used for AVO analysis. Generally, the VSP surveys mentioned above have receivers down the borehole and the sources on the surface (Stewart, 2001).

BACKGROUND

A zero offset and three walkaway multi length VSP surveys were acquired to investigate fractured lower Cretaceous coals in southern Alberta. These fractures, better known as face and butt cleat fracture systems, are permeability conduits for methane production. In general, the amount of methane gas within porous coal systems is larger than that of conventional gas around the world. However, most of the coal bed methane (CBM) systems have not been produced. Figure 1 shows a stratigraphic sequence of coal bearing formations in Alberta. Figure 2 shows the dominant stress direction in the Western Canadian Sedimentary Basin.

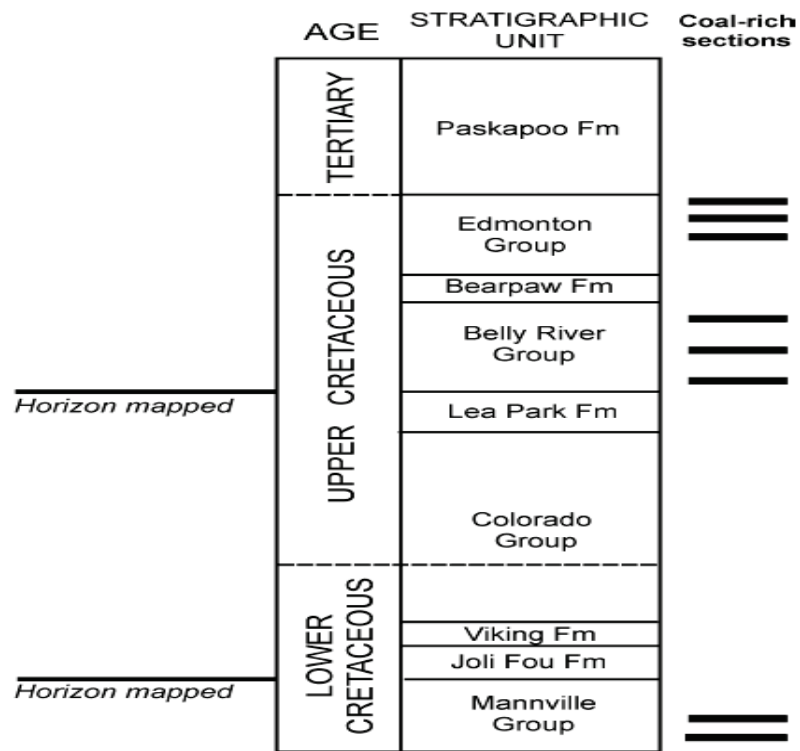


FIG.1.Stratigraphic geological sequence of coal bearing formations in Alberta (Bell and Bachu, 2003).

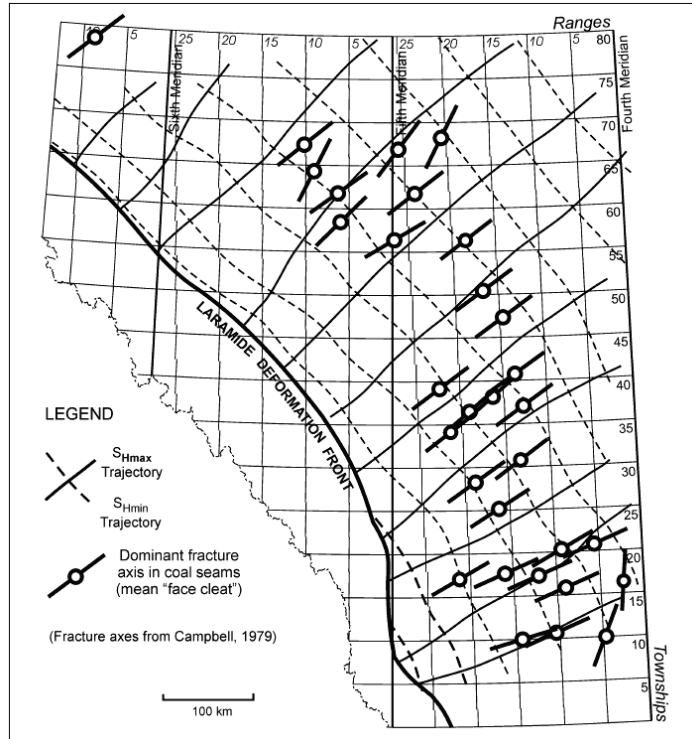


FIG.2. The maximum stress direction is NE-SW which is parallel to the face cleats (Bell and Bachu).

ZERO OFFSET VSP PROCESSING

VSP surveys have advantages over surface seismic surveys. One advantage is the ability to separate the downgoing (direct) and upgoing (reflected) wavefields that enable the calculation of true reflection amplitude or seismic impedance. The results of the calculation permit the correlation between well logs and surface seismic on one hand with the VSP result in the other. Of course, VSP data have enhanced high frequency content because waves travel through the low velocity level only once. This may help in the detection of reflectors not seen on the surface seismic data. Also, the generation of corridor stacks can help eliminated inter-bed multiples on both VSP and surface seismic data (Parker and Jones, 2008).

In VSP processing, the first step is to set up the geometry of zero-offset VSP. That enables the processor to pick first breaks which are used to flatten the data for upgoing and downgoing separation, to invert for interval velocities, for time depth conversion, and for flattening of events by doubling the first break times (Coulombe, 1993).

The next step of VSP processing is wavefield separation. There are several methods of wavefield separation including: median filtering, F-K filtering, K-L transform, tau-p transform (Hinds et al., 1999). Median filtering enhances the downgoing waves which are then subtracted from the raw data to give the upgoing waves (Coulombe, 1993).

The downgoing waves are then flattened using first break times, trace equalized to account for spherical spreading and transition losses and to avoid introducing trace-by-

trace effects to the data, then a deconvolution operator is designed. The deconvolution operator is applied to the upgoing waves and the waves are scaled by the same factor used on the upgoing waves. Reflection coefficients are then calculated from the ratio of upgoing to downgoing wave. After deconvolution, propagation effects such as some multiples are eliminated (Coulombe, 1993).

The last processing step is to shift the upgoing waves by the first break times to get two way time. Also, data are NMO corrected in the process. A corridor is used to account for propagation effects of upgoing waves, such as inter-bed multiples, and include reflections from below the well (Coulombe, 1993).

All of the VSP surveys are shown in a map view illustration Figure 3 (Parker and Jones, 2008).

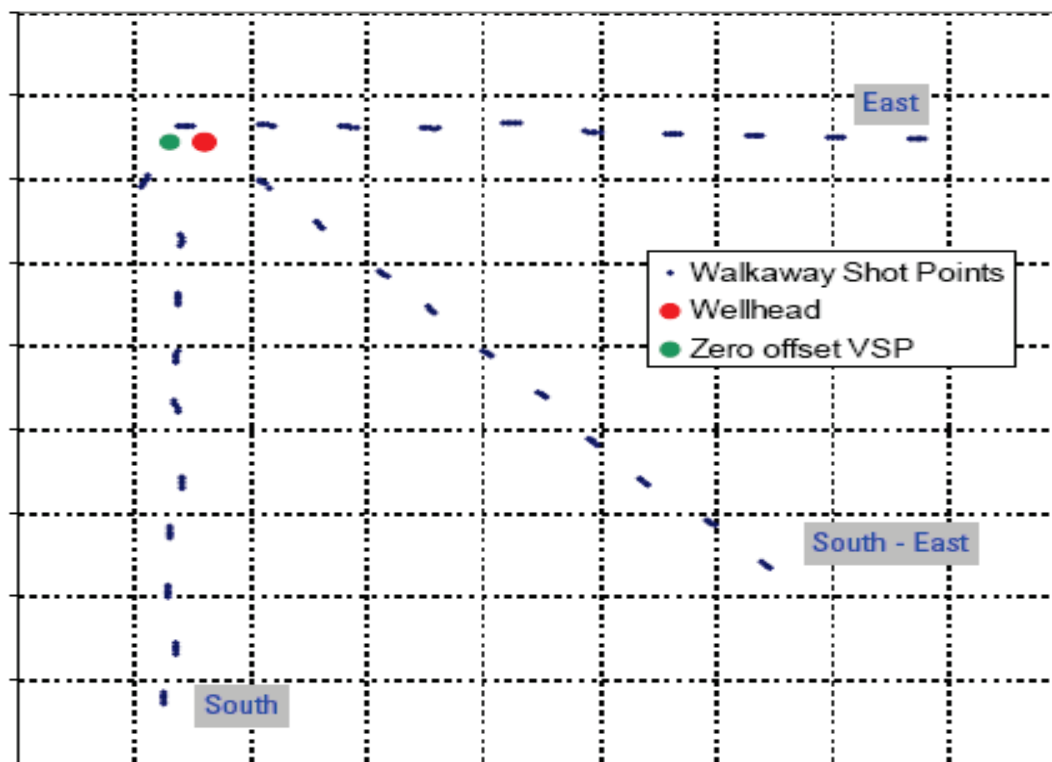


FIG.3. Shows the VSP surveys acquired in Alberta. The red dot indicates the location of the well. The green dot indicates the Zero offset VSP source location. Finally the dotted lines indicate the offset shots of the walkaway VSPs.

The zero-offset VSP was acquired by two Litton truck-mounted vibroseis units with a 62 m offset and at an azimuth of 269 degrees. A VSI tool with sixteen shuttles was used in the acquisition of the VSP data from depths 1420 – 48.7 m measured depth from Kelly bushing and 1 ms sampling rate. The receiver spacing is 15.1 m. A minimum of seven shots with sweep of 12 s consisting of frequency of 8-120 Hz were acquired with a 3 second design window. The vertical well had a Kelly bushing of 872.2 m above mean sea level (MSL) while the ground level is 868.1 m above MSL.

The zero-offset VSP was processed using VISTA. Referring to the log report, the geometry of the zero-offset VSP has been set, with channel numbers 1, 2, 3, corresponding to X, Y and Z components given Trace Code ID of 1, 3 and 2 for X, Y, Z respectively. The first break times are picked on the raw vertical Z component and displayed in Figure 4. Since this is a vertical well, the downgoing P waves in the zero offset survey dominate the energy of the wavefields.

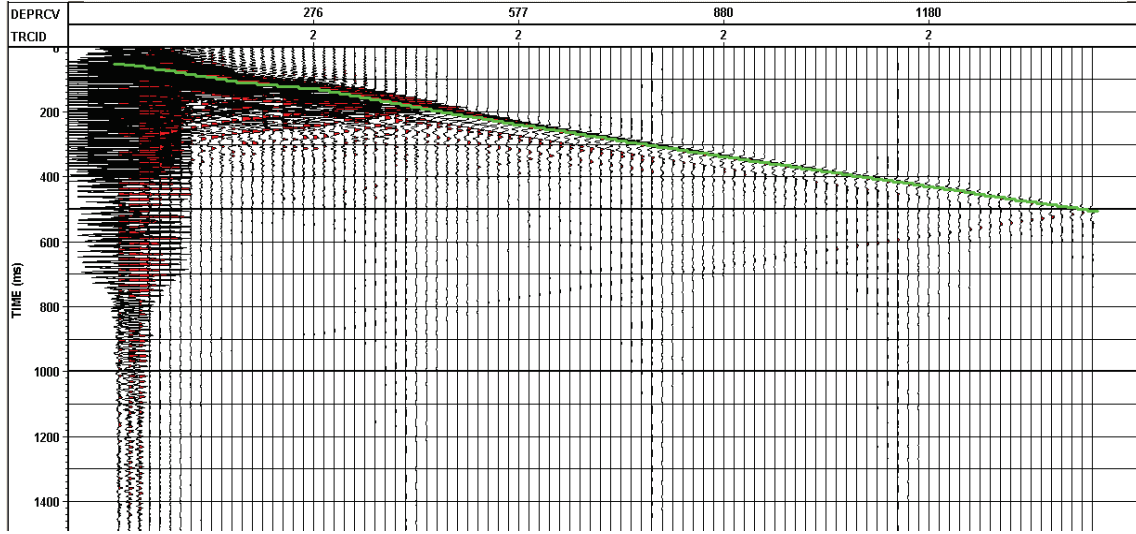


FIG. 4. Raw zero offset VSP Z component with first break times.

The first breaks were picked and the interval velocities were calculated, stored and displayed in Figure 5. The near surface replacement velocity is calculated by dividing the depth of the first receiver, 48.7 m, by the first break time of the first receiver, 0.0522 s and rounded to 950 m/s.

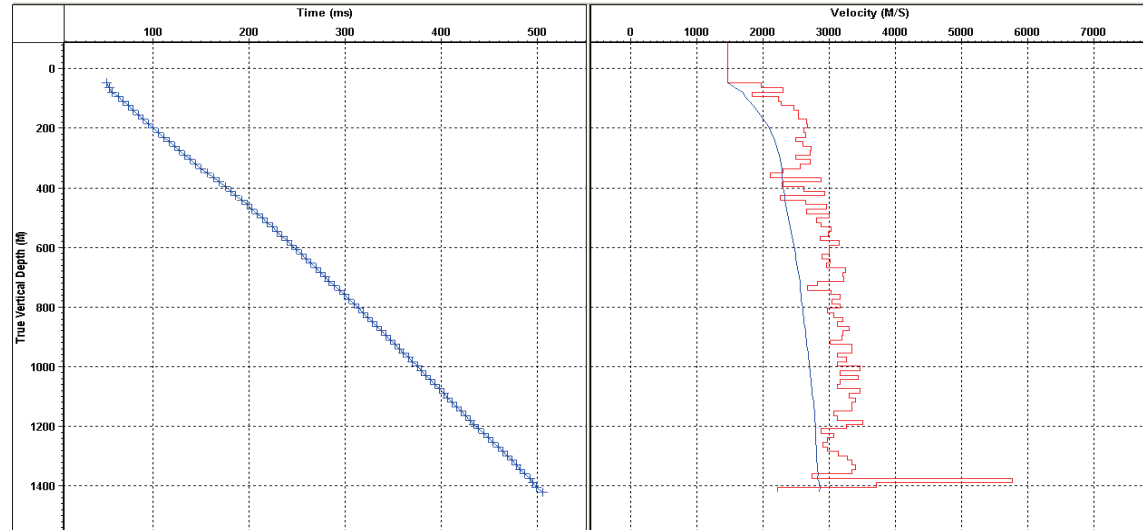


FIG. 5. The left figure shows the first break times of the raw vertical component plotted against depth. The right figure shows the corresponding interval velocities in red with rms velocity in blue.

The next major processing step was to separate the downgoing from upgoing wavefields. Median filtering is the method that I chose to separate the wavefields and tested different lengths of median filtering, which consist of 9, 11, 13, 14, 15, 19 and 21 median point filter. Median filtering is performed after selecting a point range of operation like a selection of a series of depth traces. Next, the end traces are padded and the whole range of traces is sorted depending on their magnitude strength. Later, the median trace in the middle is placed within a depth and time as the window of selected data slides to another range of traces (Hinds et al, 1999). Since there was no distinct difference in the median filtered upgoing waves, the analysis was mainly based on the isolation of the downgoing waves. In the end and with the consultation of Rick Kuzmiski, it was decided to go with 21 point median filtering since it best isolated the downgoing waves and showed the most continuous and coherent downgoing events while eliminating the upgoing waves best in the Z(-TT) section. The Z(-TT) section represents the vertical raw Z data flattened and bulk shifted to the datum. I deleted the first four traces of the median filtered 21 point median filter Z(-TT) to get a better section. Figure 6 shows the downgoing Z(-TT) wavefield after applying a 21 point median filter with 500 ms Automatic Gain Control (AGC). Figure 7 shows the resulting upgoing Z(-TT) wavefield after subtracting the downgoing waves from the original Z(-TT) wavefields with -9 db applied to the amplitudes.

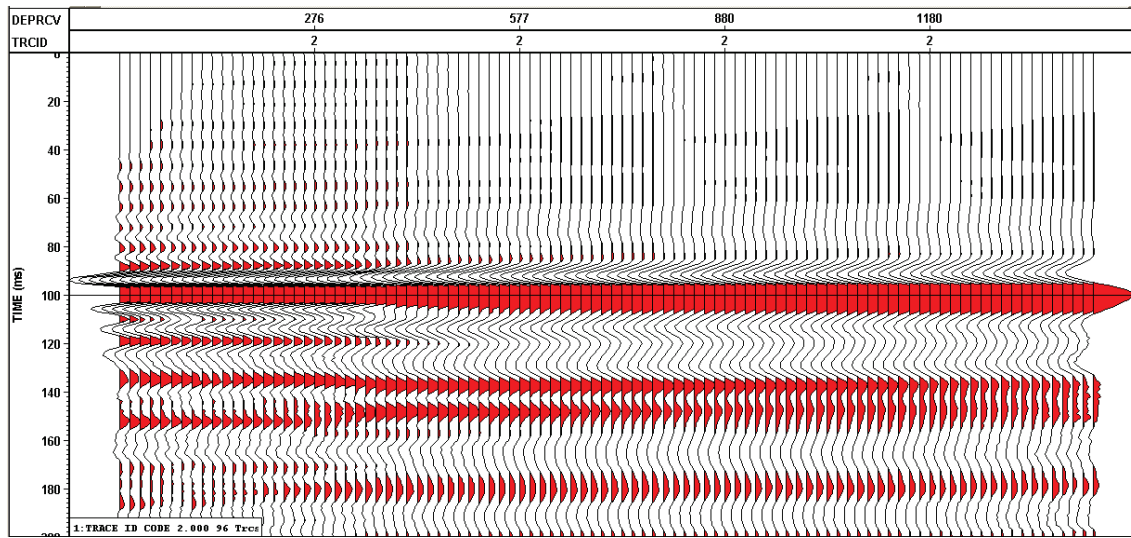


FIG. 6. Downgoing Z(-TT) with 21 point median filtering after subtracting upgoing waves.

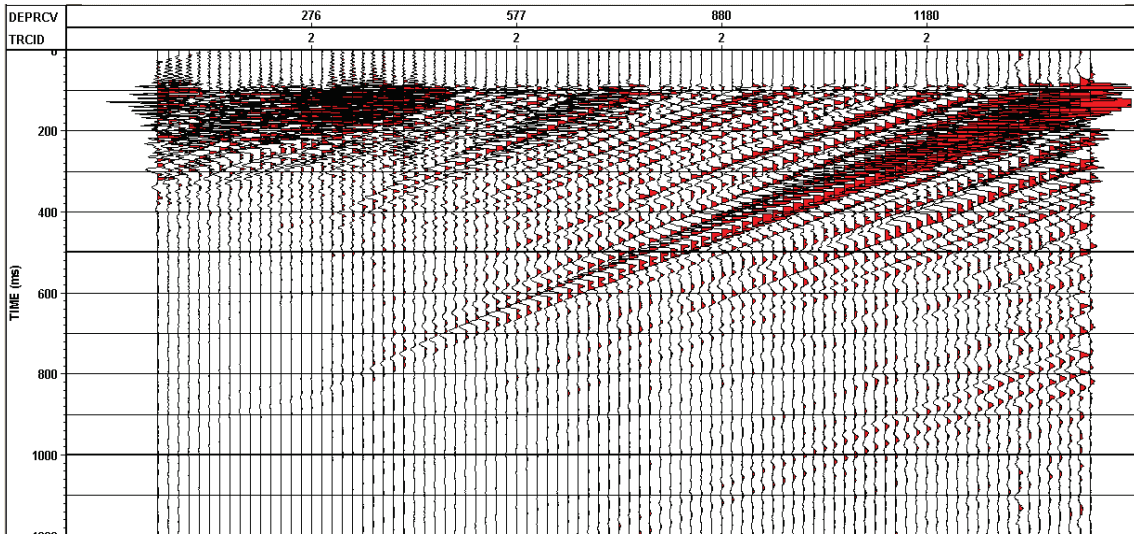


FIG. 7. Upgoing $Z(-TT)$ as a result of subtracting the 21 point median filtered $Z(-TT)$ from the original $Z(-TT)$.

The next step at this point is to deconvolve the data using the downgoing wavefield that represents the source signature and apply it to the upgoing. A division of upgoing frequency spectrum waves over downgoing frequency spectrum of waves in the FK domain creates a zero phase multiple free wavefield (Hinds et al, 1999).

The first part of the deconvolution flow has both inputs as the downgoing $Z(-TT)$ after 21 point median filtering to optimize the deconvolution parameters. The deconvolution windows started at 0 ms and extended to 1000 ms. The window is chosen because the data does not contain multiples within it. The next part of the processing of deconvolution produces the deconvolved downgoing waves that are utilized to design a deconvolution operator to be applied to the upgoing $Z(-TT)$. The second part of the deconvolution procedure has the first input as the downgoing $Z(-TT)$ after 21 point median filtering and the second input as the corresponding upgoing $Z(-TT)$. The result gives the deconvolved upgoing $Z(-TT)$ wavefield. Figure 8 shows the downgoing deconvolved wavefield while Figure 9 shows the upgoing deconvolved wavefield.

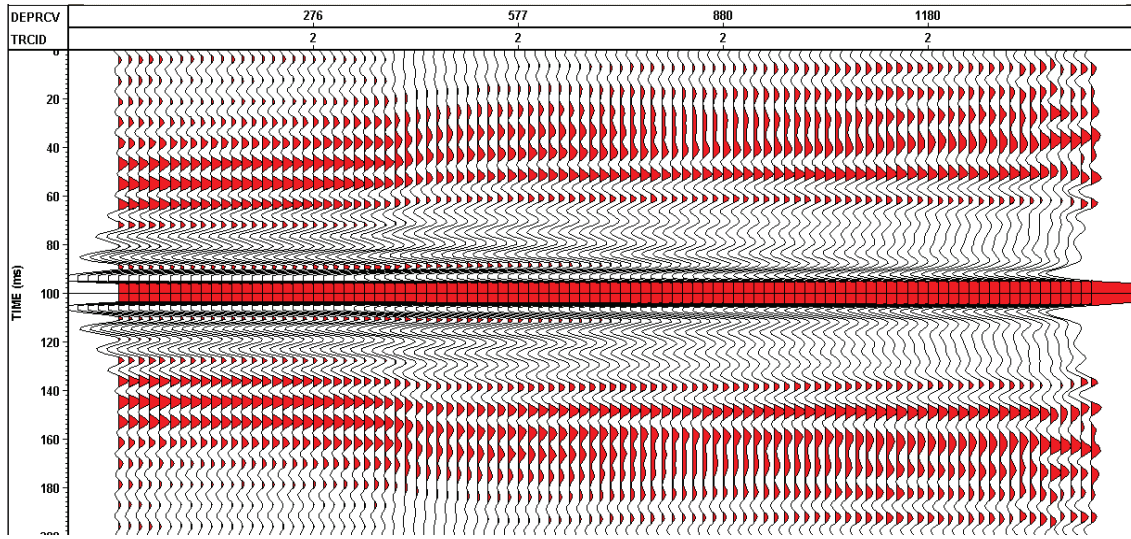


FIG. 8. The deconvolved downgoing Z(-TT) after 21 point median filtering.

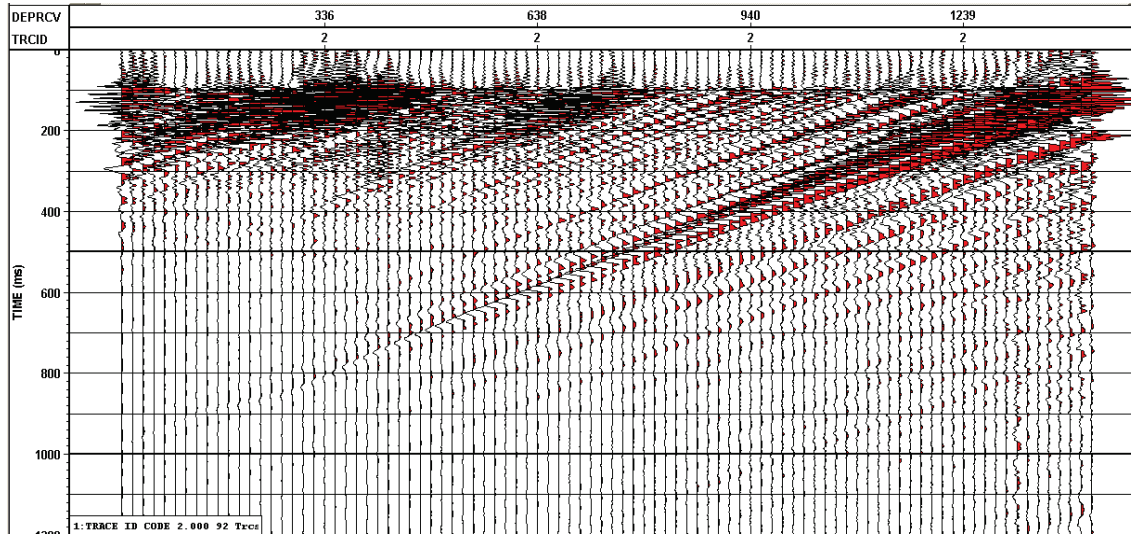


FIG. 9. The deconvolved upgoing Z(-TT) after 21 point median filtering.

Now that the data is deconvolved, the need to develop inside and outside corridor mutes is pursued. The data muted is the deconvolved upgoing median filtered Z(-TT). The flattened Z(-TT) has an exponential gain of 10 applied to it. Then the data is converted to Z(FRT) for the application of NMO correction, using the interval velocities calculated earlier from first breaks of the zero offset VSP, to ensure that events are in their proper times and will tie with surface seismic data in the future. The NMO-corrected data is then converted to two-way-time by multiplying the first break times by two. A mute is applied to ensure the correction of the VSP trace times for future true amplitude recovery. This produces the first output of Z(+TT) that is in two-way-time and NMO corrected. This result is then bandpass filtered to limit noise. The Z(+TT) and NMO corrected data are median filtered with 4 point median filtering to enhance the signal to noise ratio. Furthermore the data is bandpass filtered once more. Then the result is converted back to Z(FRT), corridor muted and converted back to Z(+TT) to produce an

inside corridor mute and an outside corridor mute. A corridor mute of 50 ms and to a depth of 1220 m is applied to the corridor muted data. Figure 10 shows the inside corridor mute while Figure 11 shows the outside corridor mute.

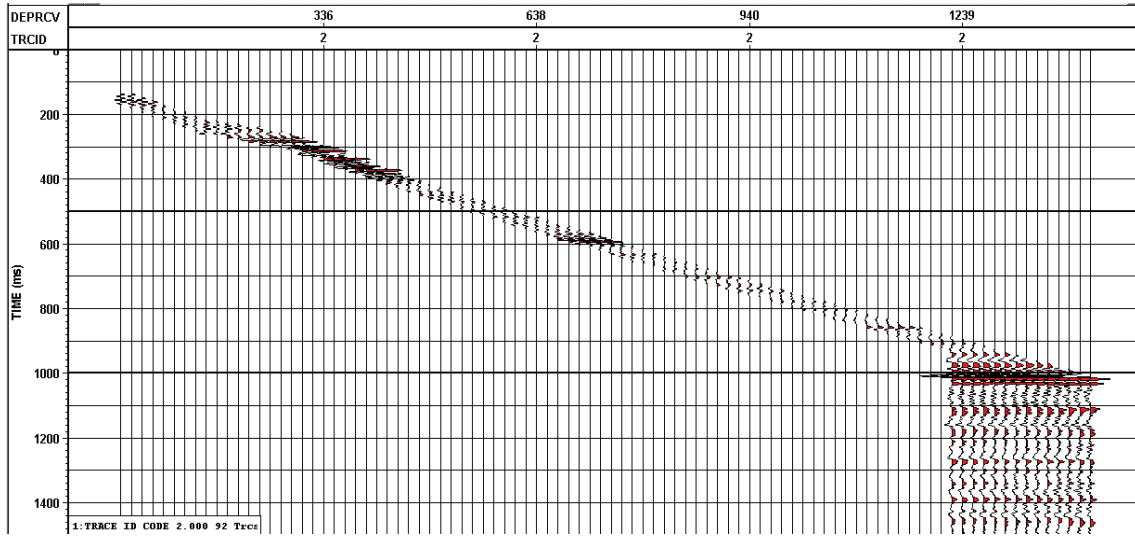


FIG. 10. Inside corridor mute of 50 ms applied to the upgoing Z(FRT) wavefield down to 1220 m of depth.

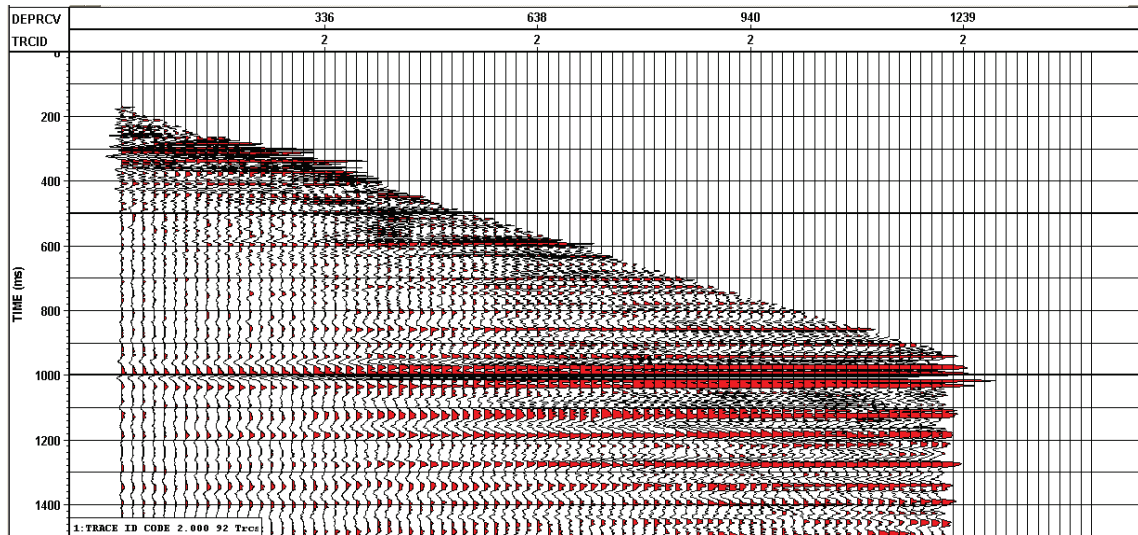


FIG. 11. Outside corridor mute of 50 ms applied to the upgoing Z(FRT) wavefield down to 1220 m of depth.

The last processing step performed on the zero offset VSP is the stacking of the corridor muted data. Figure 12 shows the outside and inside corridor stacks.

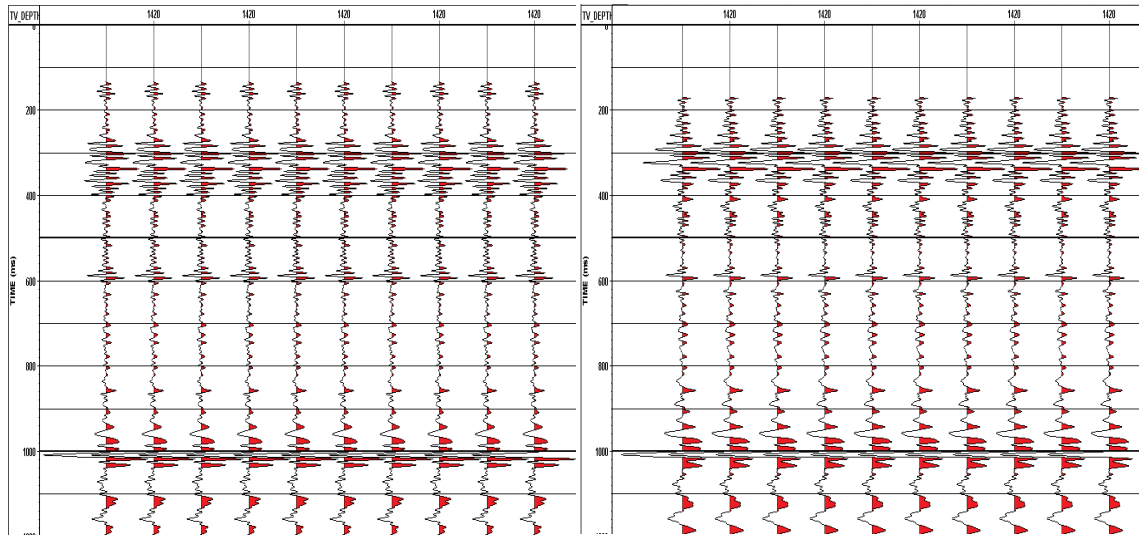


FIG. 12. VSPCDP multi offset stack of the VSP walkaway survey.

Analysis of Figure 12 shows that the zero offset VSP survey is essentially multiple free since there is little difference in the number of events between the outside and inside corridor stacks.

SOUTH WALKAWAY VSP PROCESSING

The walkaway VSP survey line processed for south of the well with 11 offsets, 51, -139, -240, -379, -518, -647, -802, -938, -1079, -1214, -1346 m. In this report, only the processing of the -647 m and the -1079 m offsets are shown. The VSP survey was acquired using dynamite as the source a 16 shuttle VSI tool with a shuttle separation of 15.1 meters. These shuttles contained three component geophones. Four shuttle tool settings were lowered into the borehole each with 16 shuttles to get a full coverage of receivers from depth 468 meters to depth 1420 meters.

The processing flow of VSP data starts with the geometry and ends with the VSPCDP stack. Similar to the zero offset VSP, the geometry and Trace Code ID are set up before the first break picks and interval velocity calculation. However, a problem was encountered with the shot statics and therefore the first break times had to be altered and bulk shifted. Figure 13 shows the first break times and interval velocities before and after the correction for offset -647 m while Figure 14 shows the same data for offset -1079 m.

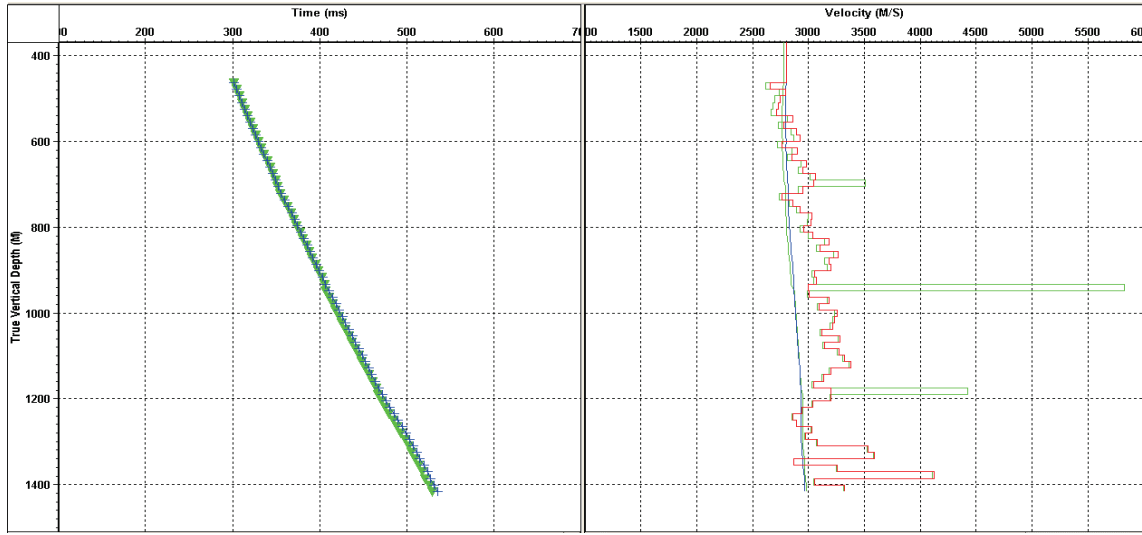


FIG. 13. First break line and interval velocity before and after shot static correction for south walkaway offset -647 Z component. The left side shows the first break lines before correction in green and after correction in blue. The right side shows the interval velocities after correction in red and before correction in green.

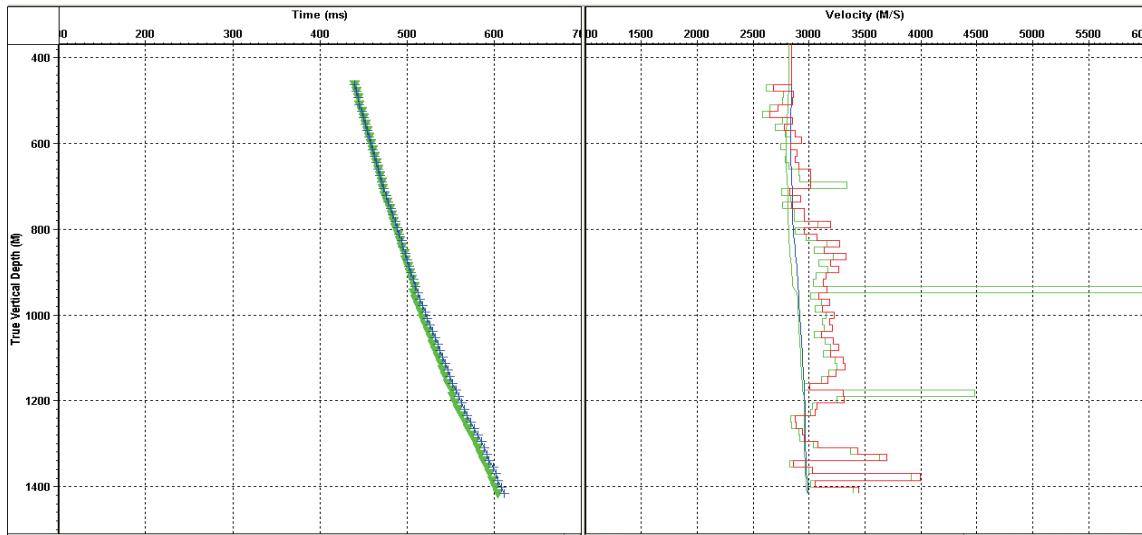


FIG. 14. First break line and interval velocity before and after shot static correction for south walkaway offset -1079 Z component. The left side shows the first break lines before correction in green and after correction in blue. The right side shows the interval velocities after correction in red and before correction in green.

Two time-invariant hodogram rotations that were applied to two horizontal components X and Y, and a time-variant rotation that is applied later to the upgoing P and SV wavefields. Considering the time-invariant rotation, the first hodogram rotation is performed on the two horizontal components X and Y to orient the data towards the source and result in Hmax and Hmin. Ideally, Hmax would contain the Primary (P) and Shear Vertical (SV) wavefields while the Hmin component would contain the SH wavefield. The second hodogram rotation orients Hmax' towards the source and the Z' in the plane of the source and orthogonal to Hmax' (Hinds et al., 1999). In theory, the

H_{max}' component would contain the downgoing P and upgoing SV while Z' would contain the downgoing SV and upgoing P wavefields. The time-invariant hodogram rotations use a least square fit to determine the angle of rotation (Hinds et al., 1999).

After the H_{max} , Z , H_{max}' and Z' components were obtained, they were FK filtered to separate the different downgoing and upgoing P and SV wavefields. In VISTA, the upgoing wavefields plot in the positive wave number domain while the downgoing waves plot in the negative wave number domain. Figures 15-22 below are the upgoing H_{max} known as upgoing SV, upgoing Z known as upgoing P, downgoing H_{max}' also known as downgoing P and downgoing Z' also known as downgoing SV.

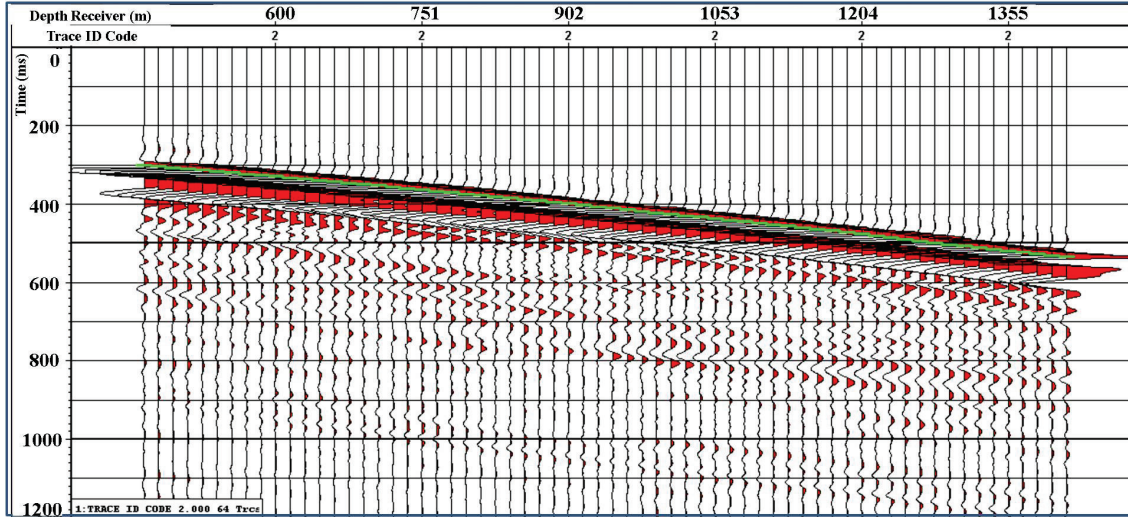


FIG. 15. South walkaway downgoing P waves for source offset -647 m.

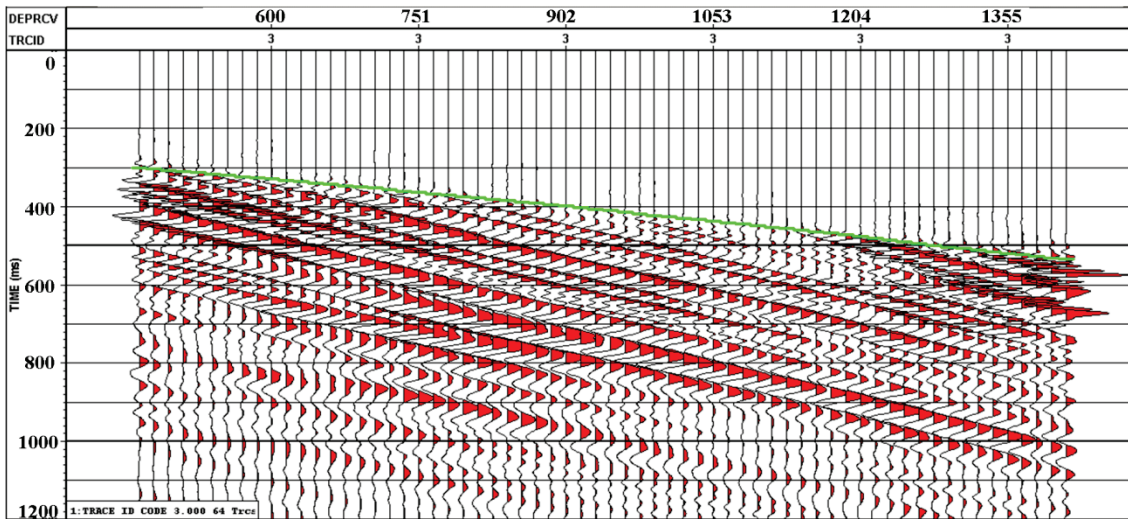


FIG. 16. South walkaway downgoing SV waves for source offset -647 m.

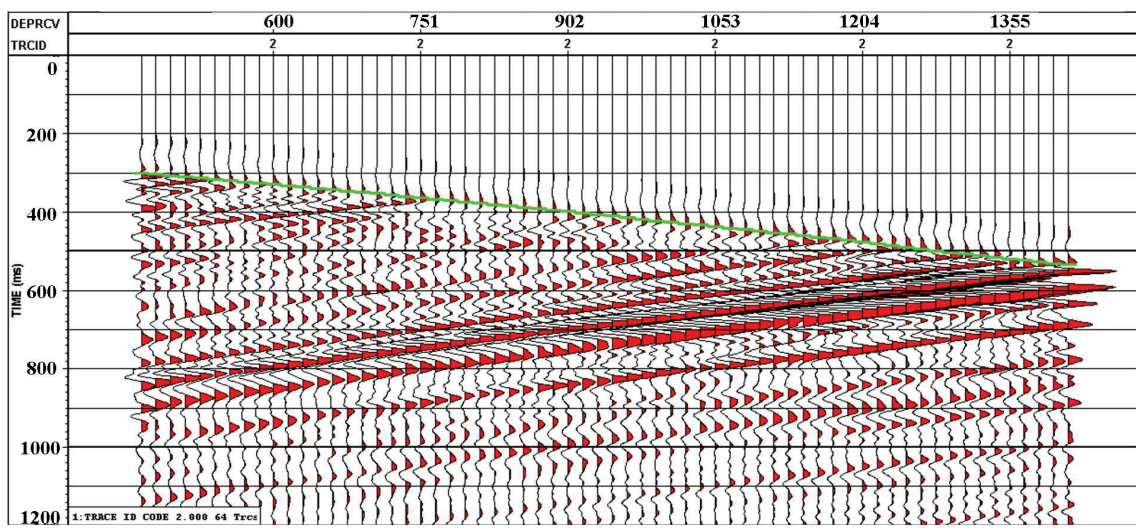


FIG. 17. South walkaway upgoing P waves for source offset -647 m.

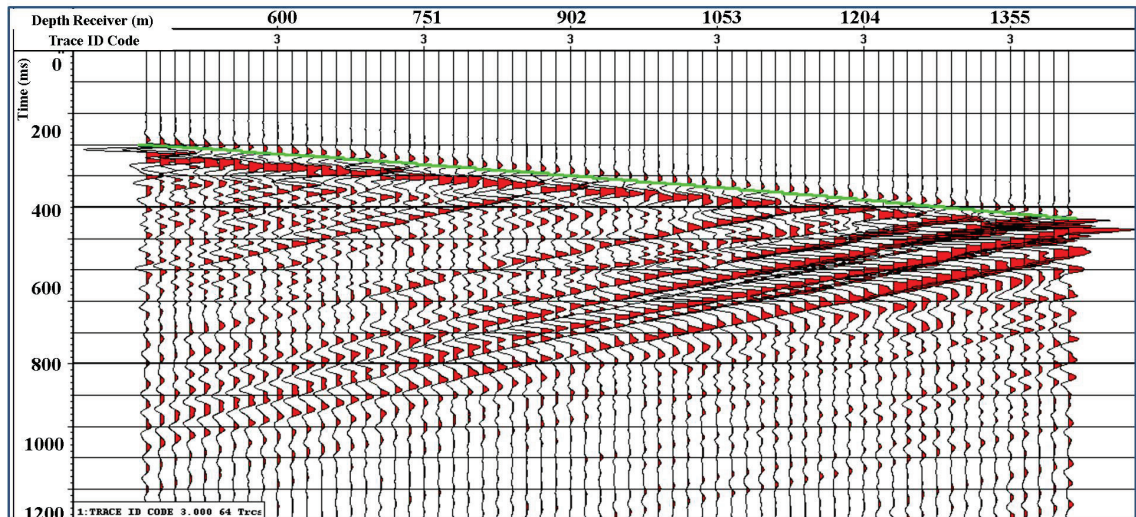


FIG. 18. South walkaway upgoing SV waves for source offset -647 m.

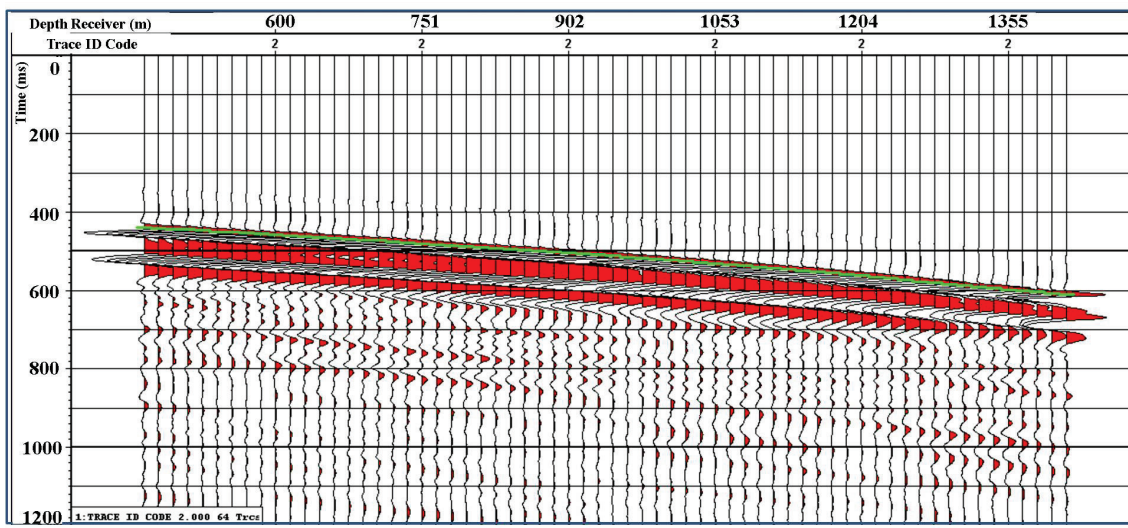


FIG. 19. South walkaway downgoing P waves for source offset -1079 m.

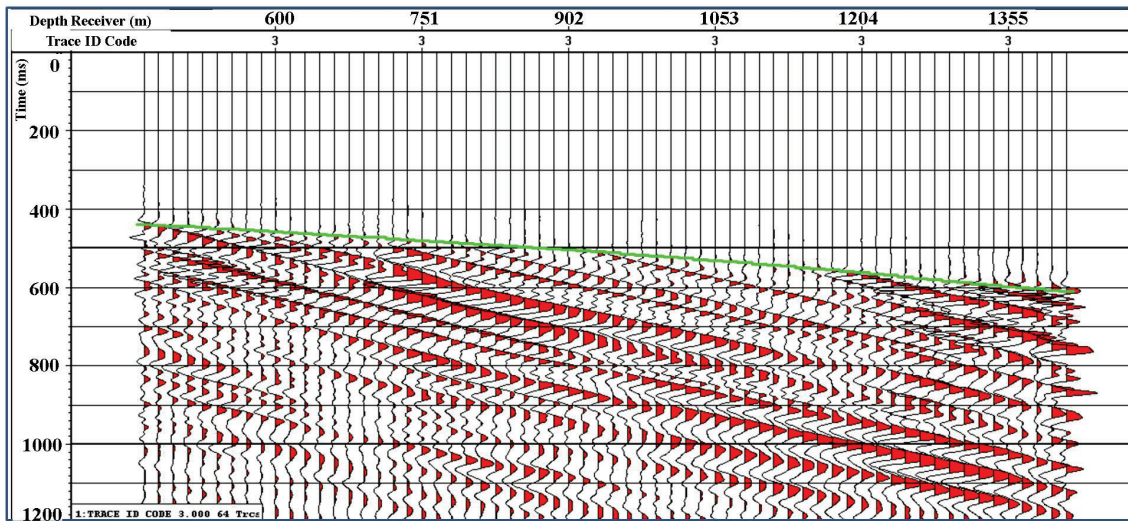


FIG. 20. South walkaway downgoing SV waves for source offset -1079 m.

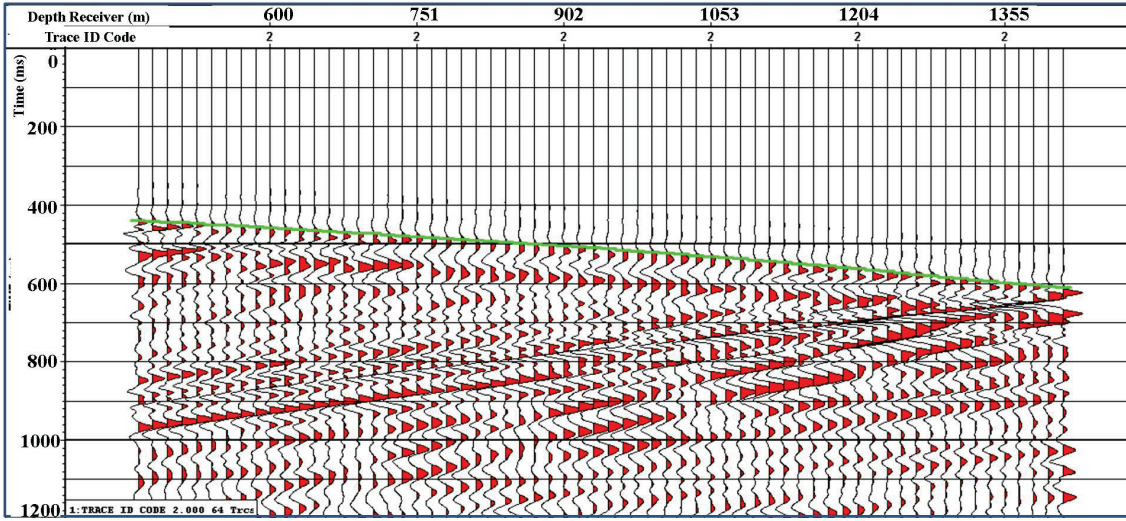


FIG. 21. South walkaway upgoing P waves for source offset -1079 m.

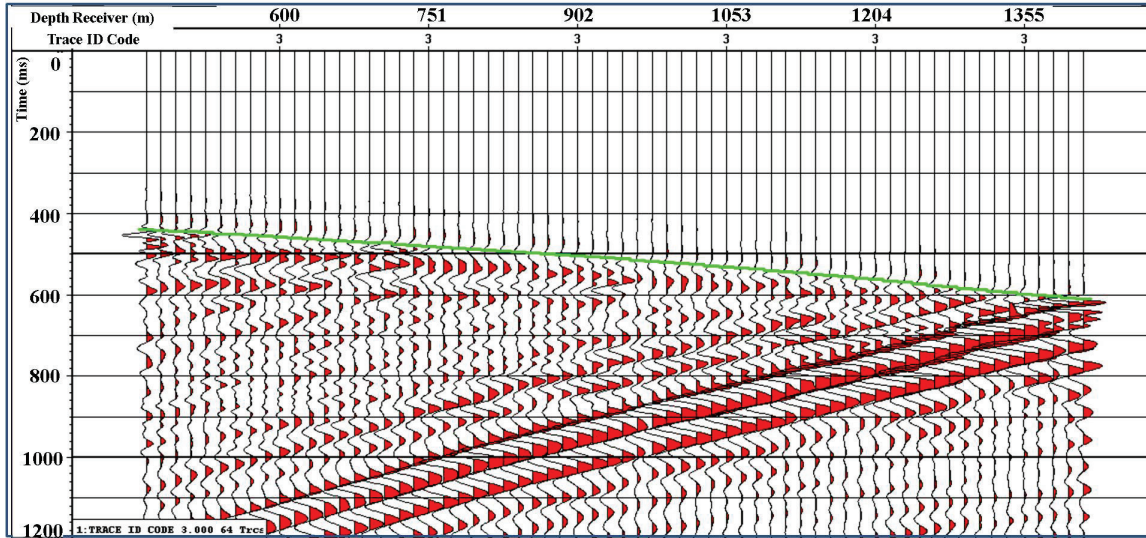


FIG. 22. South walkaway upgoing SV waves for source offset -1079 m.

After wavefield separation, SV upgoing and P upgoing wavefields are input for time variant rotation. This step polarizes P waves on one component and SV on the other. The reason behind the need for time variant rotation for P and SV isolation has to do with the change of reflection angle of different layers below a considered geophone. As a result, the angles of incidence from the reflected reflector to the upper geophone changes with time and therefore one angle of rotation is not adequate to isolate the P and SV waves (Hinds et al., 1999). Time variant rotation is done after ray tracing the events of SV upgoing and P upgoing. The ray tracing technique uses 5000 traces with angles going from 270-360 degrees. It is noted that in the time variant rotation, input 2, which is the upgoing P waves in this case, is flipped in polarity since in some cases the polarity is flipped after hodogram rotations such as the one performed on Hmax in this case. This change in polarity isolates the P and SV results in different Trace Code IDs. The only exceptions are to the flip polarity are the southeast walkaway offset -51 and the south

walkaway offset 51. Figures 23 to 26 show the P and SV upgoing waves of the two offsets after time variant rotation.

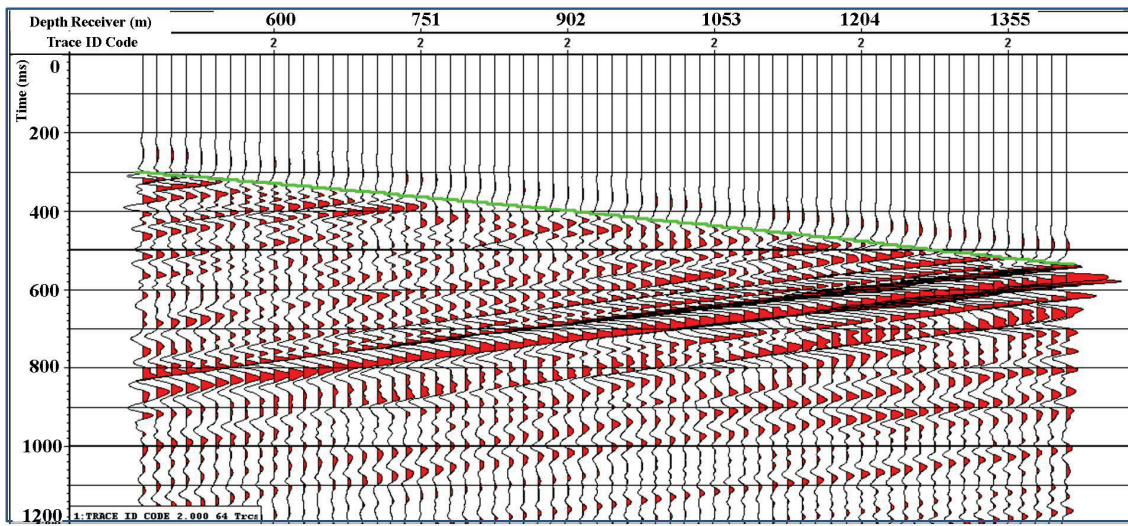


FIG. 23. South walkaway upgoing P waves after time variant rotation for source offset -647 m.

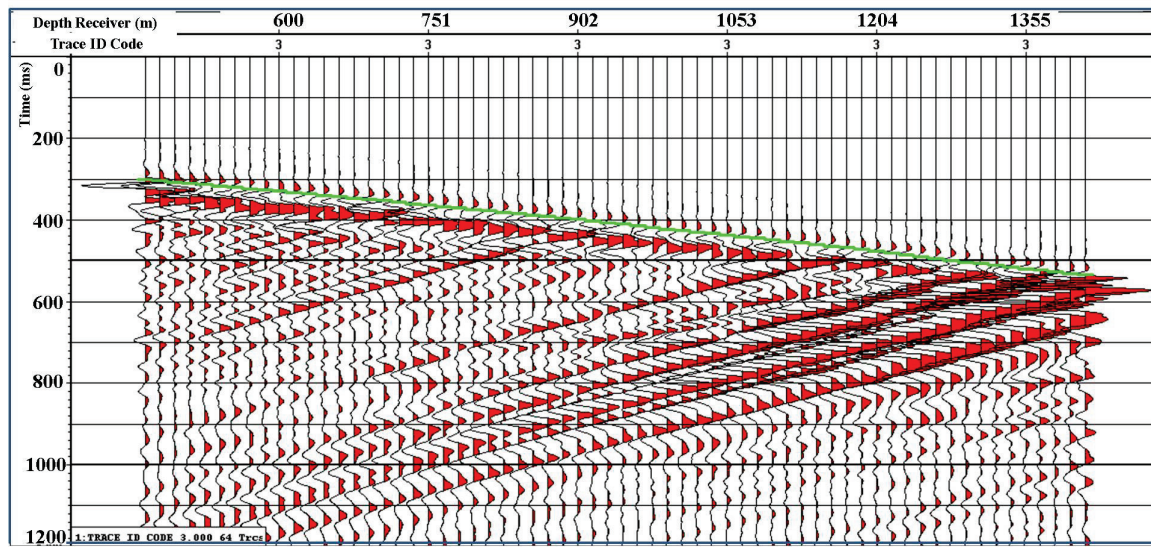


FIG. 24. South walkaway upgoing SV waves after time variant rotation for source offset -647 m.

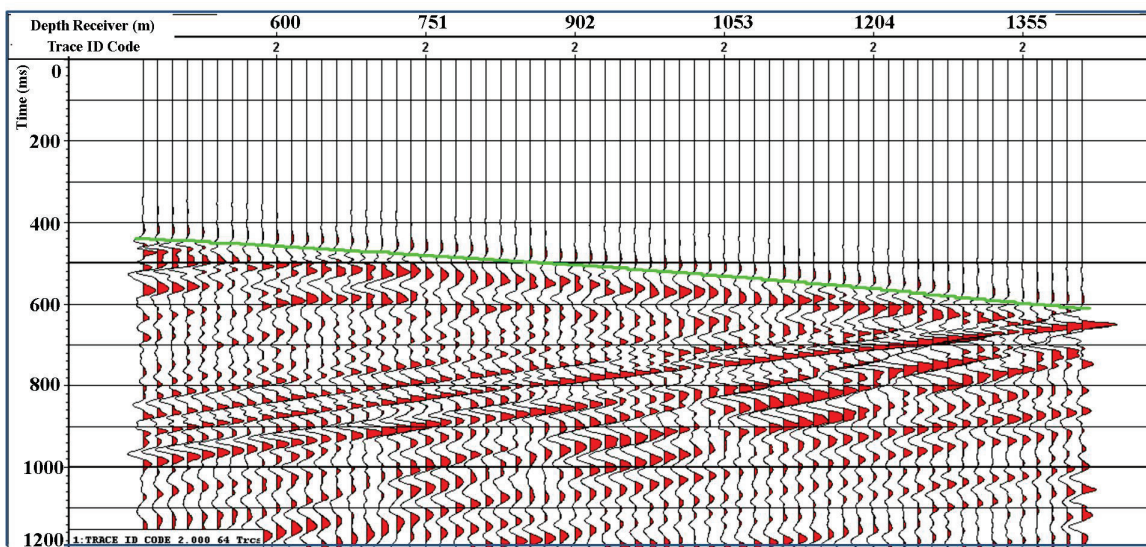


FIG. 25. South walkaway upgoing P waves after time variant rotation for source offset -1079 m.

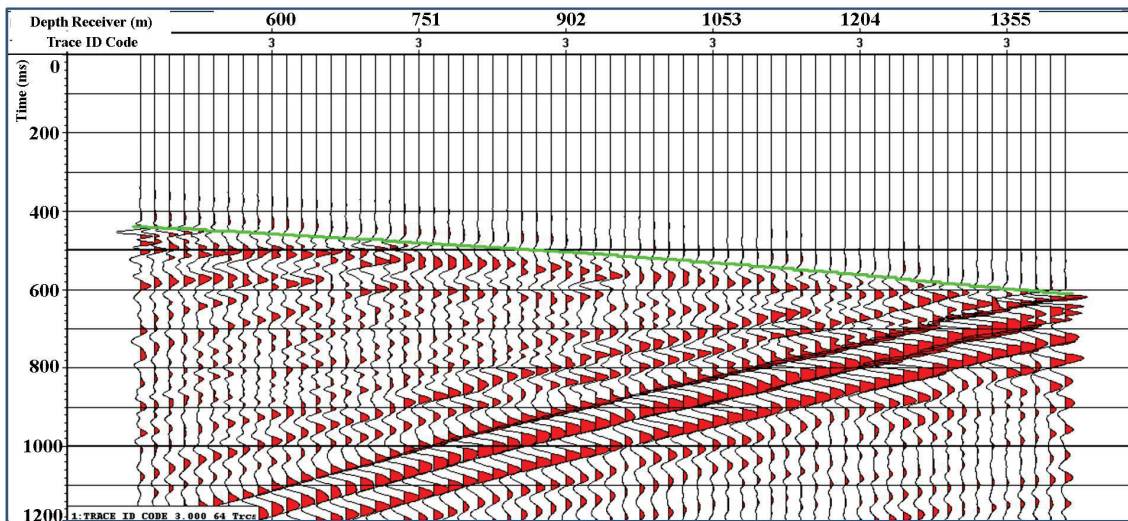


FIG. 26. South walkaway upgoing SV waves after time variant rotation for source offset -1079 m.

After separation of both P and SV upgoing wavefields, deconvolution was applied. A deconvolution window of 250 ms was chosen to apply to both the downgoing and upgoing wavefields. As with the zero offset deconvolution, the deconvolution operator is designed on the downgoing P waves and applied to the upgoing waves. A filter of 5-10-70-80 Hz was applied to the output of the deconvolution. Figures 27 to 30 show the deconvolved P and SV waves.

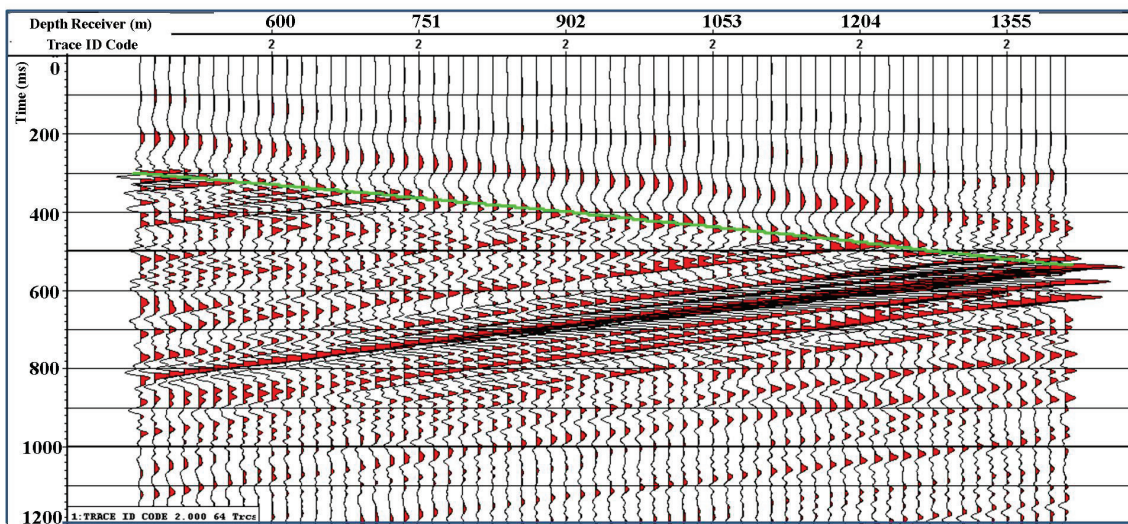


FIG. 27. South walkaway deconvolved upgoing P waves for source offset -647 m.

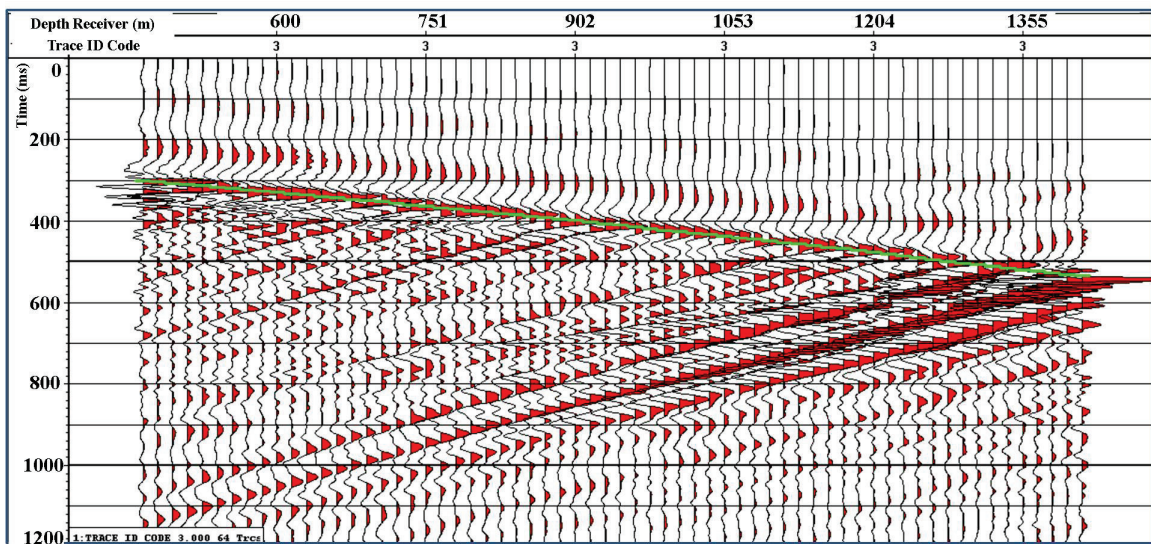


FIG. 28. South walkaway deconvolved upgoing SV waves for source offset -647 m.

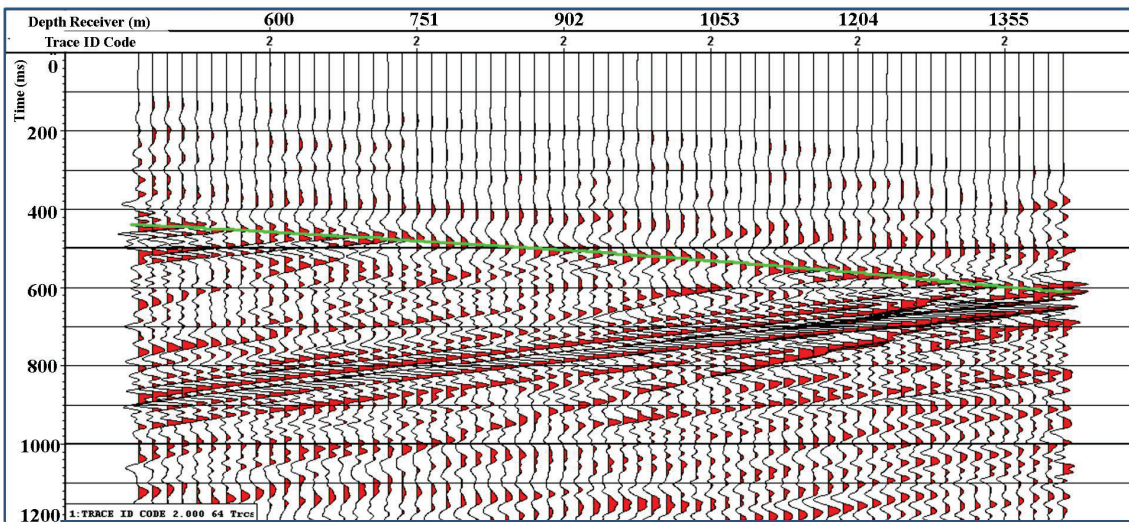


FIG. 29. South walkaway upgoing P waves for source offset -1079 m.

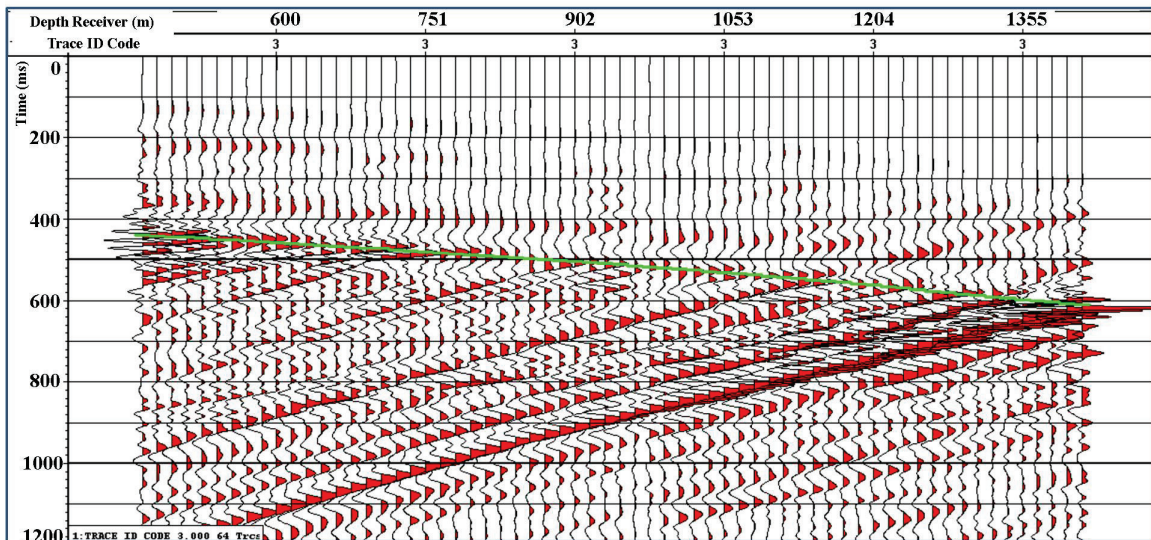


FIG. 30. South walkaway upgoing SV waves for source offset -1079 m.

The last processing step to be applied to the data is NMO correction and VSP CDP stacking. All of the offset data shots are used as input to the stacking process. The upgoing P waves from all the offsets are subject to gain and then NMO corrected using the zero offset VSP interval velocities calculated from the zero offset VSP Z raw data. The data was then filtered with a 5-10-70-80 Hz filter to reduce noise. Next a median filter of 4 points is applied to enhance signal to noise ratio. Another bandpass filter of 5, 10, 70, 80 is applied before the data is CDP stacked. Figure 31 shows the final result of stacking.

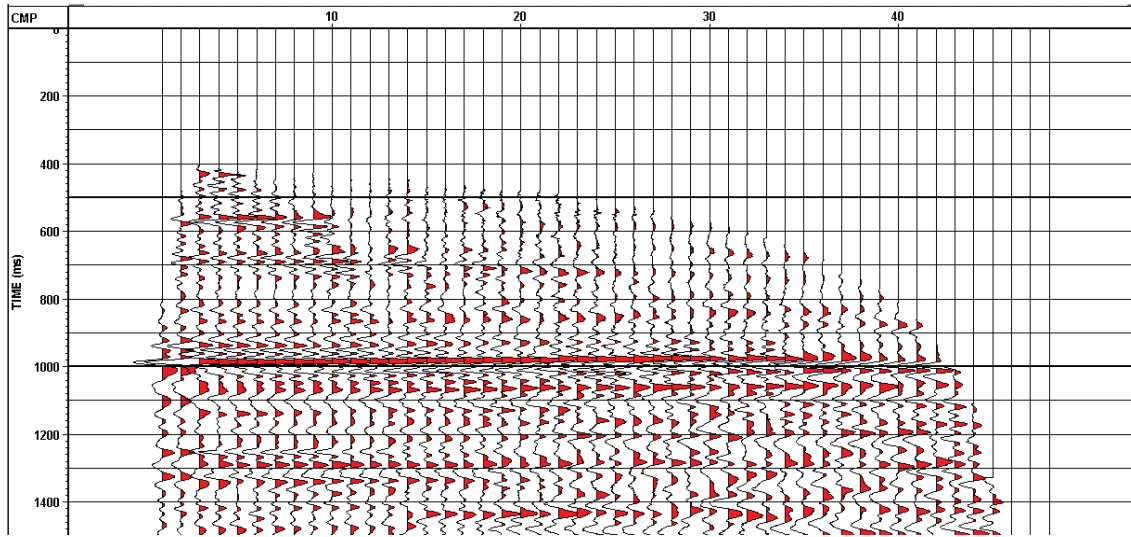


FIG. 31. South walkaway multi offset VSP CDP stack.

In the south walkaway multi offset VSP CDP it is clear that the most reflective event is the Mannville coals at 1 s time. The event is strong in the near offsets and slightly fades in the far offsets.

CONCLUSION

This report contained the steps needed to process a zero offset VSP survey and a walkaway VSP survey. Both surveys processed started with the separation of components and picking first breaks but later differed in the processing flow.

The zero offset VSP was essential and contributes to the walkaway offset VSP surveys. From the zero offset VSP I was able to obtain an interval velocity model after picking the first breaks. This interval velocity model was used later in time-variant rotation and stacking of the walkaway VSP survey. The processing of the zero offset VSP survey included wavefield separation that used a 21 point median filter that proved to be most effective. Afterwards, deconvolution was performed on the upgoing P waves that eliminated all the possible multiples contained in the data. It is noted that the zero offset VSP data did not appear to contain multiples and therefore a 1000 ms window was selected for the deconvolution. Lastly, outside and inside corridor stacks were generated which revealed that there are no significant multiples in the data.

The walkaway VSP survey required a different processing flow. Initially, the data needed to be shot static corrected due because there were problems in the first breaks and interval velocities induced by the ends of the receiver tools. A recommendation to have at least a one receiver overlap of the tools could prove to be effective in normalizing and eliminating this problem in the future. After correction, the data needed two rotations in order to polarize the data in the plane of the source and the well. Next, the data was subject to FK wavefield separation. A further step of time variant hodogram rotation was needed to isolate the upgoing P and SV wavefields into different components. Furthermore, deconvolution was performed on the different offset wavefields before VSP CDP stacking. The multi offset VSP CDP stack showed that the reflection of the

Manville coals was quite evident and was strong at near offsets and slightly weakened at far offsets for PP reflections.

AKNOWLEDGEMENTS

We would like to extend a special thanks to Rick Kuzmiski of GEDCO for offering consultation whenever needed. Also, we would like to thank the CREWES sponsors for supporting this work, particularly Encana Corporation for providing access to the VSP data and GEDCO for proving VISTA VSP processing software. We also thank Zimin Zhang, Mohammad Al-Duhailan, Kevin Hall, Dr. Rolf Mayer, Taher Sodager, Hussain Hammad and Mingyu Zhang of GEDCO and other CREWES staff for assistance. Lastly, I would like to thank Saudi Aramco for their scholarship support.

REFERENCES

- Bell., J.S., Bachu, S., 2003, In situ stress magnitude and orientation estimates for Cretaceous coal-bearing strata beneath the plains area of central and southern Alberta, *Bulletin of Canadian Petroleum Geology*, 51, No. 1, pages 1-28.
- Coulombe, C.A., 1993, Amplitude-Versus-Offset analysis using vertical seismic profiling and well log data, Master's Thesis, Department of Geology and Geophysics, The University of Calgary.
- Hinds, R.C., Anderson, N.L., Kuzmiski, R.D., 1999, *VSP Interpretive Processing: Theory and Practice*, Society of Exploration Geophysicists.
- Parker, R., Jones, M., 2008, Rig-source VSP/Sonic Calibration/Synthetics/Walkaway VSP Processing Report, Schlumberger, pages 5-14.
- Stewart., R.R., 2001, *VSP: An In Depth Seismic Understanding*, Department of Geology and Geophysics, University of Calgary, CSEG Recorder, 26, No. 7.